Analysis of a Large Database of GCL Internal Shear Strength Results

Jorge G. Zornberg, M.ASCE[1]; John S. McCartney, S.M.ASCE[2]; and Robert H. Swan Jr.[3]

Abstract: A database of 414 large-scale direct shear test results was assembled to evaluate variables governing geosynthetic clay liner (GCL) internal shear strength. The tests were conducted by a single independent laboratory over 12 years using procedures consistent with current testing standards. A wide range of GCL types, normal stresses, and shear displacement rates allowed investigation of the effect of reinforcement, pore water pressure generation, and sources of shear strength variability. Reinforced GCLs showed higher strength than unreinforced GCLs, with needle-punched GCLs performing better than stitch-bonded GCLs. Thermal locking of needle-punched GCLs was found to be effective at high normal stress, but hydration using low hydration normal stress was found to decrease the effectiveness of thermal locking. Shear-induced pore water pressures were indirectly evaluated using shear strength results from tests conducted using normal stresses above and below that corresponding to the GCL swell pressure. The peak shear strength was found to increase with decreasing shear displacement rates for high normal stresses, while the opposite trend was observed for low normal stresses. Shear strength envelopes showed a bilinear response, with a break at normal stresses consistent with the GCL swell pressure. Good repeatability of test results was obtained using the same-manufacturing-lot GCL specimens, while comparatively high variability was obtained using different-lot specimens. Peak shear strength variability was found to increase linearly with normal stress, but to be insensitive to specimen conditioning procedures. Evaluation of reinforced and unreinforced GCL test results indicates that, in addition to reinforcement variability, bentonite variability contributes to the shear strength variability of reinforced GCLs. Peel strength was found not to be a good indicator of the contribution of fibers to the GCL peak shear strength.

DOI: 10.1061/(ASCE)1090-0241(2005)131:3(367)

CE Database subject headings: Databases; Shear strength; Data analysis; Shear tests; Geosynthetic; Clay liners.

Introduction

Geosynthetic clay liners (GCLs) are prefabricated geocomposite materials used in hydraulic barriers as an alternative to compacted clay liners. They consist of sodium bentonite clay bonded to one or two layers of geosynthetic backing materials (carrier geosynthetics). Advantages of GCLs include their limited thickness, good compliance with differential settlements of underlying soil or waste, easy installation, and low cost. Stability is a major concern for side slopes in bottom liner or cover systems that include GCLs because of the very low shear strength of hydrated sodium bentonite (Mesri and Olson 1970). Proper shear strength characterization is needed for the different materials and interfaces in hydraulic barriers. In particular, the failure surface of a liner system may develop internally (within the GCL), either through its bentonite core or along the bentonite/carrier geosynthetic interface. The internal shear strength of GCLs is the focus of the study presented in this paper.

Several investigators have evaluated the GCL internal shear strength using direct shear and ring shear tests (Gilbert et al. 1996, 1997; Stark et al. 1996; Eid and Stark 1997; Fox et al. 1998; Eid et al. 1999). These experimental studies have provided invaluable insight into the significance of parameters that govern the shear behavior of GCLs. However, available information on GCL internal shear strength is still limited to specific ranges of normal stresses, GCL types, and test conditions. There are three primary reasons why a comprehensive evaluation of GCL internal shear strength is still needed. First, the use of tests from different laboratories may have masked sources of variability, as was the case in a shear strength database assembled by Stoewahse et al. (2002) using results from European laboratories. Second, the current standard for internal and interface GCL shear strength testing (ASTM D6243) has only been available since 1998 (ASTM 1998), so tests conducted before the approval of this standard may have not been consistent with current procedures. Third, significant costs (large-scale direct shear devices, long time for conditioning and testing) have limited the number of available test results and precluded evaluations of variability.

A database of 414 large-scale direct shear tests conducted by a single laboratory was assembled and evaluated in this study to identify and quantify the variables governing the internal shear strength of GCLs. This database, referred to as the GCL shear strength (GCLSS) database, is used to define upper and lower bounds on peak and large-displacement GCL internal shear strength. In addition, an analysis of the results in the GCLSS database allows evaluation of: (1) The performance of GCLs

[1]Clyde E. Lee Assistant Professor, Dept. of Civil Engineering, Univ. of Texas at Austin, 1 University Stn., C1792, Austin TX 98712-0280.

[2]Graduate Student, Dept. of Civil Engineering, Univ. of Texas at Austin, 1 University Stn., C1792, Austin TX 98712-0280.

[3]President and CEO, SGI Testing Services, Atlanta, GA.

Note. Discussion open until August 1, 2005. Separate discussions must be submitted for individual papers. To extend the closing date by one month, a written request must be filed with the ASCE Managing Editor. The manuscript for this paper was submitted for review and possible publication on October 31, 2002; approved on April 23, 2004. This paper is part of the ***Journal of Geotechnical and Geoenvironmental Engineering***, Vol. 131, No. 3, March 1, 2005. ©ASCE, ISSN 1090-0241/2005/3-367–380/$25.00.

Table 1. Summary of GCLs in the GCLSS Database

GCL label	GCL product	Description[a]	No. of tests reaching τ_p	No. of tests reaching τ_{ld}
A	Bentomat ST	Needle-punched W-NW	270	203
B	Claymax 500SP	Stitch-bonded W-W	48	5
C	Bentofix NS	Thermal-locked, needle-punched W-NW	26	26
D	Bentofix NW	Thermal-locked, needle-punched NW-NW	16	13
E	Bentofix NWL	GCL *D* with lower mass of sodium bentonite per unit area	8	8
F	Claymax 200R	Unreinforced W-W	13	13
G	Not Marketed	GCL *A* with additives to the sodium bentonite	3	0
H	Bentomat DN	Needle-punched NW-NW	18	6
I	Not Marketed	GCL *A* with adhesive strengthened reinforcements	8	0
J	Geobent	Needle-punched W-NW	4	4

[a]W=Woven carrier geotextile, NW=Nonwoven carrier geotexile.

manufactured using different types of reinforcement, (2) pore water pressures during shearing (indirect evaluation), and (3) the GCL internal shear strength variability.

Database

Data Source

The large-scale direct shear tests in the GCLSS database were performed between 1992 and 2003 by the Soil-Geosynthetic Interaction laboratory of GeoSyntec Consultants, currently operated by SGI Testing Services (SGI). SGI is an accredited testing facility with significant consistency in its testing procedures. It should be noted that procedures used for GCL direct shear tests conducted by SGI over the period 1992 to 2003 are consistent with ASTM D6243 (ASTM 1998), even though this standard was only approved in 1998. Most tests in the GCLSS database were conducted for commercial purposes and, consequently, the testing characteristics and scope was defined by project-specific requirements. A few additional tests were conducted specifically for this investigation in order to complement tests conducted using different shear displacement rates and to incorporate peel strength results in variability analyses. Test conditions reported for each series in the GCLSS database include specimen preparation and conditioning procedures, hydration time (t_h), consolidation time (t_c), normal stress during hydration (σ_h), normal stress during shearing (σ_n), and shear displacement rate (SDR).

Materials

Direct shear tests in the GCLSS database were conducted using ten commercial GCL products (nine reinforced, one unreinforced). Table 1 provides the designation of the GCLs used in this study (GCL *A* to *J*), the product name, and a short description of the reinforcement characteristics and carrier geotextiles. An important objective of this study is the comparison of shear strength results among different types of GCLs. Unreinforced GCLs are used in applications where high shear strength is not required, while reinforced GCLs (e.g., stitch-bonded needle-punched GCLs) are used otherwise. The unreinforced GCL investigated in this study (GCL *F*) consists of an adhesive-bonded bentonite layer held between two woven polypropylene geotextiles. The stitch-bonded GCL investigated in this study (GCL *B*) consists of a bentonite layer stitched using synthetic yarns between two woven polypropylene carrier geotextiles. The needle-punched GCLs investigated in this study (GCLs *A*, *C*, *D*, *E*, *G*, *H*, *I*, and *J*) consist of a bentonite layer between two (woven or nonwoven) carrier geotextiles that is reinforced by pulling fibers through using a needling board. The fiber reinforcements are typically left entangled on the surface of the top carrier geotextile. Since pullout of the needle-punched fibers from the top carrier geotextile may occur during shearing (Gilbert et al. 1996), some needle-punched GCL products (GCLs *C*, *D*, and *E*) were thermal locked to minimize fiber pullout. Thermal locking involves heating the GCL surface to induce bonding between individual reinforcing fibers as well as between the fibers and the carrier geotextiles (Lake and Rowe 2000). For simplicity, thermal-locked needle-punched GCLs will be referred to simply as thermal-locked GCLs in this paper.

Testing Equipment and Procedures

The large-scale direct shear tests conducted in this study used large direct shear devices each containing a top and bottom shear box. Typically, the top shear box measured 305 mm by 305 mm in plan and 75 mm in depth. The bottom shear box measured 305 mm by 355 mm in plan and 75 mm in depth. For the GCL internal direct shear tests, the bottom shear box was sectioned down to plan dimensions of 305 mm by 305 mm. A constant SDR was applied to the bottom shear box using a mechanical screw drive system and the resultant shear load was measured on the top shear box using a load cell. The direct shear devices used in this study were capable of applying normal stresses from 2.4 to 3,000 kPa during shearing. Dead weights were placed above the GCL in tests conducted under low normal stresses, while an air bladder or a hydraulic cylinder were used to exert a normal force between the GCL and a reaction frame in tests conducted under relatively high normal stress. A load cell was used to measure the normal load. The accuracy of the normal stress application device and calibration of the load cells were verified at least every year as a part of a laboratory accreditation program.

A detail of the specimen configuration for GCL internal shear strength testing is shown in Fig. 1(a). A water bath may be used for testing GCLs under submerged conditions, although most tests in the GCLSS database were conducted without a water bath. For each test, a fresh GCL specimen was trimmed from the bulk GCL sample. The internal strength testing of the GCL specimen involved constraining the GCL specimen so that shearing could only occur within the bentonite component of the GCL. The specimen was constrained by bonding the two carrier geotextiles to porous rigid substrates using textured steel gripping surfaces. Extensions of each carrier geotextile were secured using a second

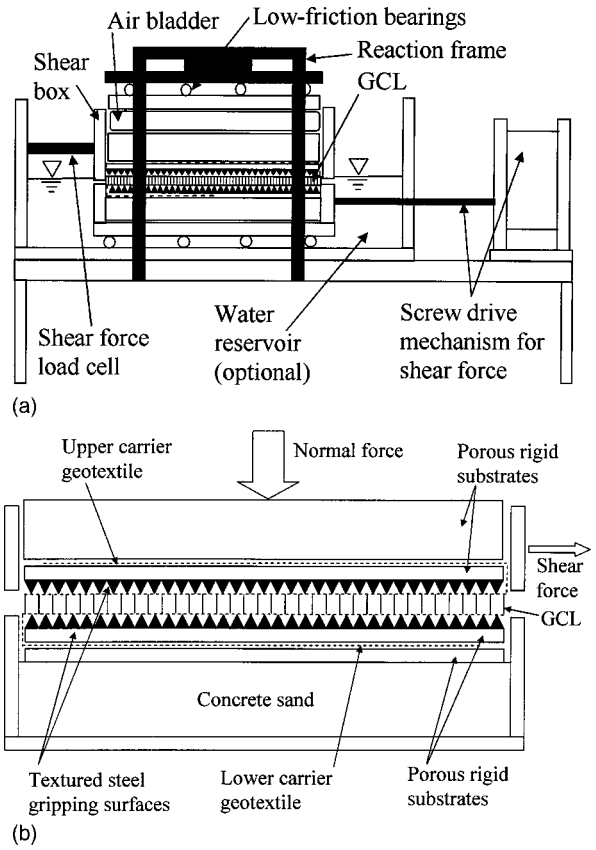

Fig. 1. Direct shear device: (a) Load application configuration; and (b) specimen detail

porous rigid substrate as shown in Fig. 1(b). The textured steel gripping surfaces were employed to minimize slippage between each carrier geotextile and the porous rigid substrate. Post-test examination of the sheared GCLs indicated that slippage did not occur between the GCL and the grips, suggesting a uniform shear stress transfer onto the GCL specimens.

Conditioning of specimens plays an important role in GCL internal shear strength testing as moisture interactions should simulate correctly those anticipated in the field. GCL conditioning involves hydration and (in some cases) subsequent consolidation of the sodium bentonite. Pore water pressures in the sodium bentonite of the GCLs tested in this study are negative for typical initial (as received) moisture conditions. Hydration of the sodium bentonite leads to reduction of the negative pore water pressures and vertical swelling. Changes in pore pressures and vertical deformations were not measured during GCL conditioning or shearing. Although this is consistent with the current state of the practice and ASTM (1998), measurements of vertical deformation during specimen conditioning and shearing would have allowed assessment of bentonite hydration by using conventional methods to estimate the degree of consolidation (Gilbert et al. 1997). Consequently, hydration of the bentonite was only assessed in this study by the reported hydration time. Although hydration times as high as 250 hs may be required to reach full hydration, hydration times beyond 72 hs have been reported not to significantly increase the GCL water content, especially under high σ_n (Stark and Eid 1996). The hydration process used in this study involved typically a two-stage procedure similar to that reported by Fox et al. (1998). The specimen and rigid substrates were placed under a specified σ_h outside the direct shear device and soaked in tap water during the specified t_h. This assembly was then transferred to the direct shear device. σ_h was often specified to equal the shearing normal stress (σ_n). However, if σ_h was less than σ_n (e.g., to simulate field conditions representative of bottom liners), the normal stress was slowly ramped up to σ_n, and pore pressures were allowed to dissipate during a consolidation period (t_c).

Shearing was conducted after GCL conditioning by applying the shear load under a constant SDR. The shear force was recorded for increasing shear displacement. The maximum shear stress was identified as the peak shear strength (τ_p), and the shear stress at the end of testing was identified as the large-displacement shear strength (τ_{ld}). Table 1 shows the number of tests used to define τ_p and τ_{ld} of each GCL. τ_{ld} was reported only when the post-peak shear stress reached an approximately constant value within the maximum displacement of the test device (75 mm). In some cases, shearing was discontinued after reaching the peak value because the test, conducted for commercial purposes, did not require post-peak assessment. In other cases, a peak shear strength value was reached, but partial separation of the reinforcements from the carrier geotextiles after reaching the peak led to an unrealistically high τ_{ld}, especially at low normal stress. As will be discussed below, the particular mode of shear failure of stitch-bonded GCL *B* generally did not allow shearing beyond the peak value.

SDR in the field is anticipated to occur slowly, which is consistent with drained conditions (Gilbert et al. 1997). The SDR used for most tests in the GCLSS database is 1.0 mm/min. While relatively fast for guaranteeing drained conditions, a SDR of 1.0 mm/min is typically used in engineering practice because of time and cost considerations. Additional tests were sheared using slower rates (as low as 0.0015 mm/min). Shearing was typically terminated when a displacement of 75 mm, or an approximately constant τ_{ld} value, was reached. Consistent with observations reported by Gilbert et al. (1996) and Fox et al. (1998), dismantling of the needle-punched thermal-bonded and unreinforced GCL specimens indicated that failure occurred typically through the interface between the bentonite and the carrier geotextile. The carrier geotextiles were always found to contain extruded bentonite. In the stitch-bonded GCL *B* specimens, the continuous fibers stretched during initial shearing. However, once the continuous fibers became fully stretched, continued shear displacement often led to rupture of the fibers or tearing of the carrier geotextiles at the threaded connections. Despite the particular arrangement of fiber reinforcements in stitch-bonded GCLs, observation of the specimens after testing did not show slippage of the woven geotextiles at the interface with the gripping system.

Analysis of Results from Different GCL Materials

A total of 32 failure envelopes (FEs) were defined considering the different GCL types and test conditions used in this investigation. A total of 385 of the 414 test results were used, while 29 test results did not have similar conditioning procedures to any of the 32 defined failure envelopes. Table 2 summarizes the test conditions, the approximate range of σ_n, and the friction angle and cohesion intercept defining the τ_p and τ_{ld} envelopes. In some cases, the internal shear strength was also characterized using a bilinear FE. The square root of the mean-squared error of the linear regression, which is considered the standard deviation of the linear regression (Helsel and Hirsh 1991), was calculated as a measure of the spread of data around the best-fit lines:

Table 2. Summary of Failure Envelopes in the Geosynthetic Clay Liner Shear Strength (GCLSS) Database

			Test conditions					Peak				Large-displacement[b]			
Failure envelope[a]	GCL label	Number of tests	SDR (mm/min)	σ_h (kPa)[c]	t_h (hs)	t_c (hs)	σ_n range (kPa)	c_p (kPa)	ϕ_p (Degrees)	R^2	s (kPa)	c_{ld} (kPa)	ϕ_{ld} (Degrees)	R^2	s (kPa)
FE 1	*A*	27	1.0	σ_n	24	0	3.4–72	13.5	46.6	0.987	3.11	2.1	8.6	0.842	1.25
FE 2	*A*	2	1.0	4.8	24	0	14–24	10.7	37.1	1.000	N/A	3.3	4.0	1.000	N/A
FE 3	*A*	12	0.5	σ_n	24	0	48–386	42.8	24.6	0.975	11.00	9.4	9.8	0.968	4.78
FE 4	*A*	40	1.0	σ_n	48	0	2.4–2759	42.4	14.0	0.966	25.36	16.2	6.3	0.983	12.49
FE 4 (Low σ_n)	*A*	31	1.0	σ_n	48	0	2.4–97	14.4	35.4	0.948	13.04	N/A	N/A	N/A	N/A
FE 4 (High σ_n)	*A*	9	1.0	σ_n	48	0	97–2759	102.4	11.9	0.987	52.78	N/A	N/A	N/A	N/A
FE 5	*A*	5	1.0	4.8	48	0	14–276	35.9	29.9	0.991	6.79	2.0	4.4	0.996	N/A
FE 6	*A*	8	1.0	σ_n	72	0	2.4–103	17.4	34.7	0.840	10.80	2.8	8.5	0.943	1.93
FE 7	*A*	141	0.1	20.7	168	48	35–310	20.6	25.2	0.999	23.88	15.5	9.4	0.999	10.65
FE 8a	*A*	1	0.0015	8.0	144	1,476	248								
FE 8b	*A*	1	0.0015	63.0	48	540	520	74.3	21.9	0.988	23.38	35.0	5.8	0.991	5.22
FE 8c	*A*	1	0.0015	8.0	144	2,328	993								
FE 9	*A*	3	1.0	68.9	24	12	138–552	37.9	22.7	0.998	5.53	2.8	11.2	0.918	17.69
FE 10	*A*	3	1.0	6.9	60	24	4.8–29	12.4	50.1	0.991	1.98	N/A	N/A	N/A	N/A
FE 11	*A*	7	1.0	0.0	0	0	2.4–35	12.9	60.1	0.921	4.64	N/A	N/A	N/A	N/A
FE 12	*B*	7	1.0	σ_n	24	0	24–690	53.4	7.3	0.818	16.93	N/A	N/A	N/A	N/A
FE 13	*B*	25	1.0	4.8	48	0	2.4–982	24.3	4.4	0.949	3.87	N/A	N/A	N/A	N/A
FE 14	*B*	10	1.0	7.2	96	0	10–1000	24.1	4.6	0.976	5.21	N/A	N/A	N/A	N/A
FE 15	*B*	3	0.1	20.7	168	48	35–310	32.4	7.3	0.994	1.95	N/A	N/A	N/A	N/A
FE 16	*C*	13	0.5	σ_n	24	0	7.2–575	23.3	23.8	0.959	13.08	12.3	9.8	0.951	11.12
FE 16 (Low σ_n)	*C*	6	0.5	σ_n	24	0	7.2–103	17.2	28.3	0.999	12.07	N/A	N/A	N/A	N/A
FE 16 (High σ_n)	*C*	7	0.5	σ_n	24	0	103–575	9.7	14.9	0.950	14.41	N/A	N/A	N/A	N/A
FE 17	*C*	10	0.2	55.2	24	0	10–290	22.0	29.3	0.993	5.17	8.0	12.0	0.975	3.86
FE 18	*C*	3	0.1	20.7	168	48	35–310	22.3	16.6	1.000	0.21	0.9	8.3	0.974	4.67
FE 19	*D*	6	1.0	σ_n	72	0	6.9–552	5.7	18.6	1.000	5.28	0.1	8.4	0.985	5.21
FE 20	*D*	3	0.5	σ_n	24	0	98–380	75.3	25.1	0.997	0.20	21.3	9.6	0.982	5.43
FE 21	*D*	6	0.1	3.4	24	24	6.9–690	40.9	27.1	0.972	27.40	15.5	8.0	1.000	0.18
FE 21 (Low σ_n)	*D*	3	0.1	3.4	24	24	6.9–28	22.4	38.9	0.972	2.03	N/A	N/A	N/A	N/A
FE 21 (High σ_n)	*D*	3	0.1	3.4	24	24	172–690	101.0	21.6	1.000	2.03	N/A	N/A	N/A	N/A
FE 22	*E*	4	1.0	σ_n	336	0	14–58	32.7	31.8	0.993	1.20	7.3	11.3	0.994	0.37
FE 23	*E*	4	1.0	σ_n	48	0	14–58	30.6	38.9	0.993	1.57	6.8	13.7	0.993	0.46
FE 24	*F*	3	1.0	σ_n	168	0	14–55	1.7	12.3	0.999	0.18	2.1	8.5	1.000	0.00
FE 25	*F*	3	1.0	0.0	0	0	69–483	16.1	3.7	1.000	0.28	10.1	4.0	1.000	1.13
FE 26	*G*	4	1.0	σ_n	24	0	2.4–19	4.8	30.4	1.000	0.11	N/A	N/A	N/A	N/A
FE 27	*H*	6	1.0	σ_n	24	0	4.8–483	19.7	33.8	0.997	8.29	23.8	5.3	0.997	1.56
FE 27 (Low σ_n)	*H*	4	1.0	σ_n	24	0	4.8–48	5.3	47.0	0.998	1.60	N/A	N/A	N/A	N/A
FE 27 (High σ_n)	*H*	2	1.0	σ_n	24	0	241–483	8.5	31.7	1.000	N/A	N/A	N/A	N/A	N/A
FE 28	*H*	6	1.0	3.4	24	24	6.9–690	33.0	32.1	0.988	21.12	29.9	8.5	0.996	3.46
FE 28 (Low σ_n)	*H*	3	1.0	3.4	24	24	6.9–28	16.5	45.0	0.971	2.58	N/A	N/A	N/A	N/A
FE 28 (High σ_n)	*H*	3	1.0	3.4	24	24	172–690	78.9	28.4	1.000	3.13	N/A	N/A	N/A	N/A
FE 29	*H*	6	0.25	0.0	96	24	4.8–10	12.1	46.3	1.000	1.63	N/A	N/A	N/A	N/A
FE 30	*I*	4	1.0	0.0	0	0	2.4–24	19.3	58.2	0.988	5.01	N/A	N/A	N/A	N/A
FE 31	*I*	4	1.0	2.4	72	0	2.4–24	21.9	51.1	0.932	1.56	N/A	N/A	N/A	N/A
FE 32	*J*	4	1.0	σ_n	24	0	24–193	5.5	9.1	1.000	0.31	0.4	6.9	0.982	1.51

[a]FE 4, 16, 21, 27, and 28 represented using both linear and bilinear envelopes.

[b]N/A=Not applicable.

[c]$\sigma_h=\sigma_n$ means that the normal stress used during hydration is the same as the normal stress used during shearing.

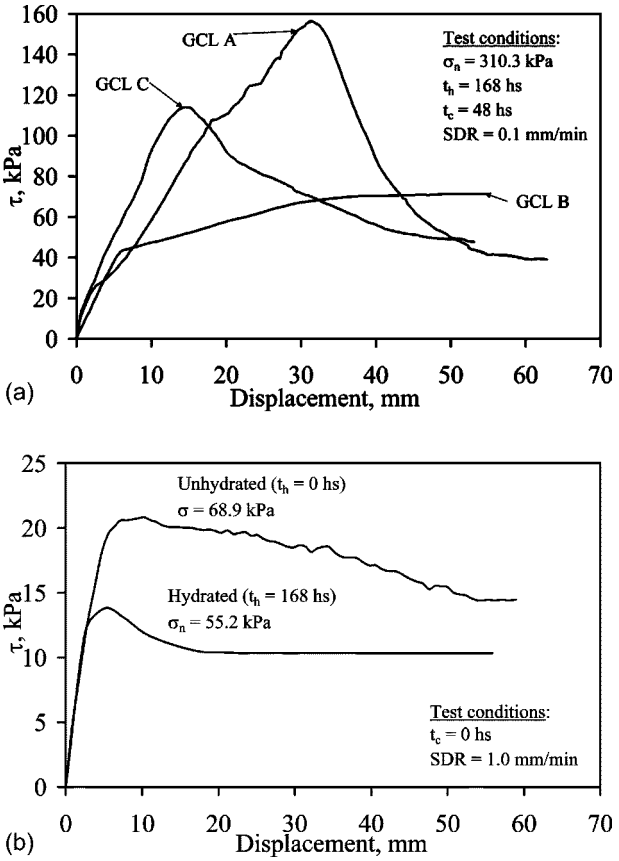

Fig. 2. Shear stress-displacement curves for different GCLs: (a) GCLs *A* (needle punched), *B* (stitch bonded), and *C* (thermally locked); and (b) GCL *F* (unreinforced)

$$s = \sqrt{\frac{\sum_{i=1}^{n} e_i^2}{n-2}} \quad (1)$$

where s=standard deviation of the linear regression; e_i=difference between the shear strength value and the value on the best-fit line at the same normal stress; and n=number of data points in the regression. Since the data summarized in Table 2 follow approximately a normal distribution around the FEs, a bound of one standard deviation contains 84% of the likely shear strength values (Helsel and Hirsh 1991).

The effect on the GCL internal shear strength of the type of internal reinforcements is investigated in this section in order to provide: (1) An evaluation of the shear stress-displacement behavior of the different GCL types, (2) a preliminary overview of GCL internal shear strength, and (3) a comparison of GCLs tested under similar conditioning procedures.

Shear Stress-Displacement Behavior

Fig. 2(a) shows shear stress-displacement curves for GCLs *A* (needle punched), *B* (stitch bonded), and *C* (thermal locked). The three GCL types were tested using the same σ_n (310.3 kPa), same t_h (168 h), same t_c (48 h), and same SDR (0.1 mm/min.). GCL *A* shows a well-defined τ_p and a marked post-peak shear strength loss. Unlike GCL *A*, GCL *B* shows a rapid initial mobilization of shear strength until reaching a "yield" stress level, beyond which a less pronounced hardening takes place until reaching τ_p. The

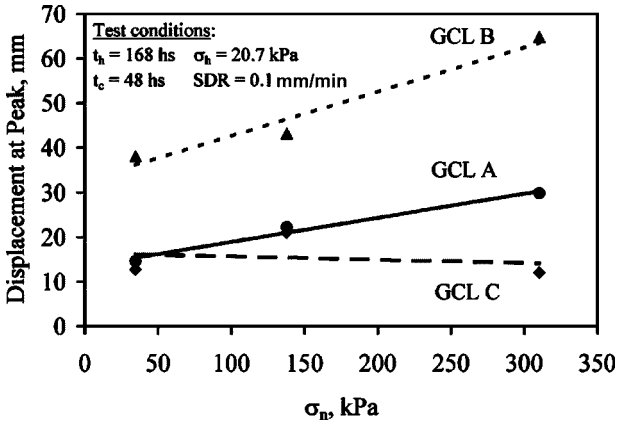

Fig. 3. Displacement at peak shear strength as a function of σ_n for GCLs *A*, *B*, and *C*

displacement at peak for GCL *B* is significantly larger than that observed for GCL *A*. The post-peak behavior of GCL *B* could not be evaluated since this GCL did not reach a steady large-displacement strength value at the maximum displacement of the device. Thermal-locked GCL *C* shows a behavior similar to that of needle-punched GCL *A*, although the τ_p value is below that obtained for GCL *A*. GCLs *A* and *C* were reinforced using similar needle-punching techniques and have the same specified peel strength (6.5 N/m). Consequently, differences in their behavior are attributed to the effect of thermal locking. Comparison of the response of the two GCLs, tested under identical conditions, suggests that thermal locking did not lead to the expected increase in shear strength.

Fig. 2(b) shows shear stress-displacement curves for GCL *F* (unreinforced) tested under hydrated and unhydrated conditions. Although a direct comparison of τ_p is not possible as the specimens were tested using different σ_n, the results indicate that the hydrated GCL has lower τ_p and τ_{ld} than the unhydrated GCL. Both specimens, however, show a significantly lower τ_p than that obtained for reinforced GCLs. The displacement at peak of unreinforced GCLs is consistent with displacement at the yield stress observed for GCL *B*. However, the displacement at peak of unreinforced GCLs is significantly lower than the one obtained for the reinforced GCLs. While both hydrated and unhydrated unreinforced GCLs show post-peak shear strength loss, the hydrated GCL appears to reach residual conditions at lower shear displacement than the unhydrated GCL.

Fig. 3 summarizes the displacement at peak for the three tests shown in Fig. 2(a) along with results from additional tests conducted under two additional σ_n values (34.5 and 137.9 kPa). GCLs *A* and *B* show increasing displacement at peak with increasing σ_n, while the displacement at peak for GCL *C* is apparently insensitive to σ_n. GCL *B* shows significantly larger displacement at peak than the other GCL types, which may be particularly relevant for displacement-based stability analyses (e.g., for seismic design). For example, if the design criterion requires a maximum shear displacement of 50 mm for a σ_n=310.3 kPa, the results in Fig. 2(a) indicate that τ_p would govern the design if GCL *B* is selected, but τ_{ld} would need to be considered if GCLs *A* or *C* are used.

Overall Internal Strength Assessment

Fig. 4(a) shows the τ_p data for all GCLs in the GCLSS database, illustrating the wide range of normal stresses at which the GCLs

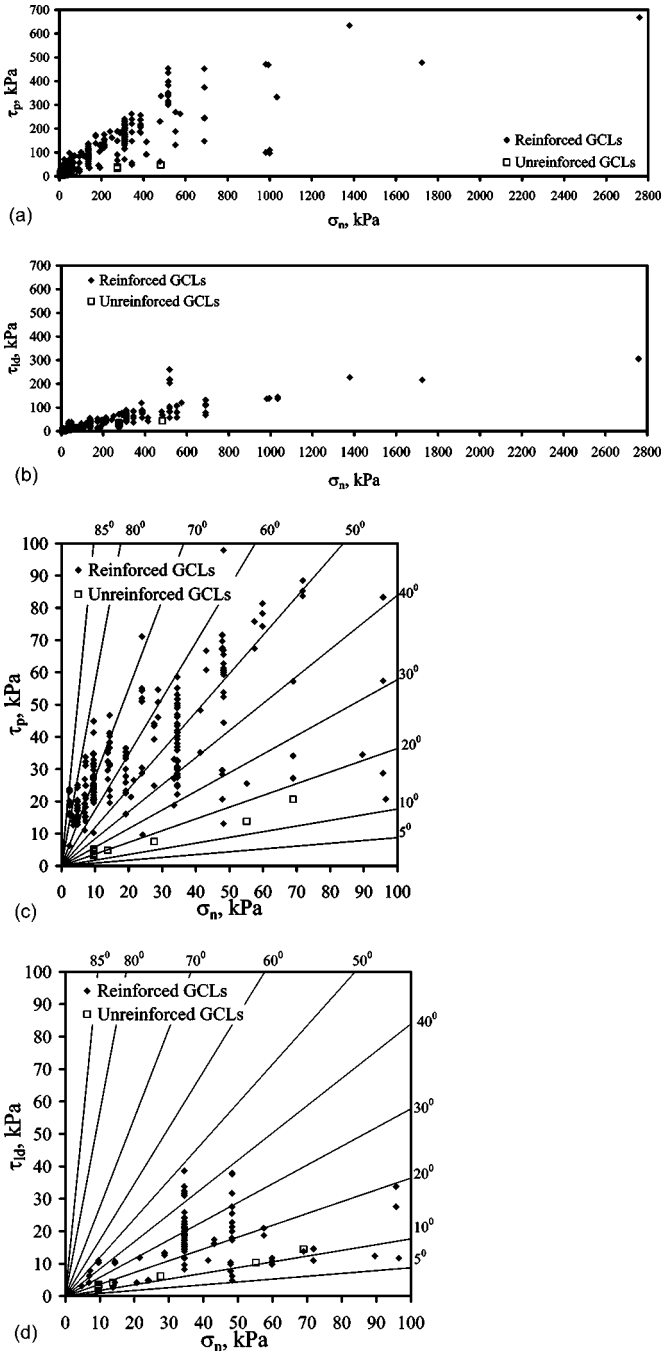

Fig. 4. Shear strength results for all geosynthetic clay liners: (a) peak shear strength values; (b) large-displacement shear strength values; (c) peak shear strength (scaled); and (d) large-displacement shear strength (scaled)

were tested and the significant scatter in the data. Similarly, Fig. 4(b) shows the τ_{ld} data for all GCLs in the GCLSS database, illustrating that the range of τ_{ld} values is significantly narrower than the range of τ_p values. As most data points shown in Figs. 4(a and b) correspond to comparatively low σ_n, Figs. 4(c and d) show a detail for σ_n values below 100 kPa. The results shown in Fig. 4(c) reflect the relevance of using a cohesion intercept to characterize τ_p at low σ_n. Inspection of the standard deviation s values in Table 2 indicates that the $s(\tau_p)$ for unreinforced GCLs (FE 24 and 25) is less than that for reinforced GCLs. Fig. 4(d) shows that the trend in τ_{ld} for low σ_n is consistent with the trend observed for higher σ_n. Inspection of the results in Figs. 4(b and d), as well as the information presented in Table 2 indicates that large-displacement shear strength is approximately independent of the GCL type. Reinforced GCLs tend to show a higher large-displacement shear strength value than the unreinforced GCLs, with stitch-bonded GCLs having the lowest large-displacement shear strength among all reinforced GCLs.

The test results for all GCLs were grouped into ten data sets based on reinforcement type. Table 3 summarizes the information for each data set, and provides the parameters for the shear strength envelopes (c,ϕ) of each data set. The GCL data sets are used only for preliminary database analysis, as they do not account for the effect of specimen conditioning on shear strength. Comparisons of τ_p values among the ten GCL data sets is aided by defining the shear strength values calculated using the GCL data set envelopes at given reference normal stresses. Table 3 includes the values of τ_{50} and τ_{300} for each data set, which are the average shear strength values at $\sigma_n=50$ and 300 kPa, respectively. These reference normal stresses are representative of normal stress values for landfill cover and liner systems, respectively. In order to quantify the variability of the shear strength for each GCL data set, the range of shear strength values was defined for each reference normal stress. Specifically, the lowest and highest shear strength values were defined using the individual failure envelopes (FE in Table 2) of each data set. Additional information is provided by McCartney et al. (2002). Inspection of the τ_{50} and τ_{300} values shown in Table 3, leads to the following observations regarding the internal peak shear strength of GCLs under low and high normal stresses:

- The peak internal shear strength of all GCLs in the database (Set SS1) can be characterized by a cohesion intercept of 38.9 kPa and a friction angle of 18.0°. However, there is a significant scatter in the results both under comparatively low normal stresses (τ_{50} ranges from 13 to 71 kPa) and comparatively high normal stresses (τ_{300} ranges from 36 to 241 kPa). The most frequently tested GCL in the GCLSS database is GCL *A* (Set SS2, 270 tests), which has peak internal shear strength that can be characterized by a cohesion intercept of 46.6 kPa and a friction angle of 18.7°. Less scatter is observed in the shear strength of GCL *A* than that observed for all GCLs both under comparatively low normal stresses (τ_{50} ranges from 48 to 66 kPa) and high normal stresses (τ_{300} ranges from 117 to 195 kPa).
- As expected, the peak internal shear strength of reinforced GCLs (Set SS3) in consistently higher than that of unreinforced GCLs (Set SS4) both under low normal stresses [τ_{50}(Set SS3)=57 kPa and τ_{50}(Set SS4)=10 kPa] and high normal stresses [τ_{300}(Set SS3)=139 kPa and τ_{300}(Set SS4)=35 kPa].
- The peak internal shear strength of needle-punched GCLs (Set SS5) is consistently higher than that of stitch-bonded GCLs (Set SS6) both under low normal stresses [τ_{50}(Set SS5)=58 kPa and τ_{50}(Set SS6)=33 kPa] and high normal stresses [τ_{300}(Set SS5)=149 kPa and τ_{300}(Set SS6)=58 kPa]. The difference is less significant under low normal stresses because stitch-bonded GCLs show some cohesion (c_p=28.5 kPa), but is more significant under high normal stresses due to the low friction angle (ϕ_p=5.6°).
- The peak internal shear strength of needle-punched GCLs with woven-nonwoven (W-NW) carrier geotextile configurations (Set SS7) is similar to that of needle-punched GCLs with NW-NW carrier geotextiles (Set SS8) under low normal stresses [τ_{50}(Set SS7)=58 kPa and τ_{50}(Set SS8)=58 kPa].

Table 3. Geosynthetic Clay Liner (GCL) Data Sets for Overall Shear Strength Assessment

GCL data set	GCL set description[a]	GCL label	Peak envelope		Peak strength at $\sigma_n = 50$ kPa	Peak strength at $\sigma_n = 300$ kPa	Large-displacement envelope	
			c_p (kpa)	ϕ_p (Degrees)	τ_{50}[range][b,c] (kpa)	τ_{300}[range][b,c] (kPa)	c_{ld} (kPa)	ϕ_{ld} (Degrees)
SS1	All GCLs	*A-J*	38.9	18.0	55[13(FE24) to 71(FE23)]	137[36(FE25) to 241(FE28)]	17.2	7.8
SS2	GCL *A*	*A*	46.6	18.7	63[48(FE7) to 66(FE1)]	148[117(FE4) to 195(FE8)]	17.2	7.6
SS3	All reinforced GCLs	*A-E*, *G-J*	40.9	18.0	57[14(FE32) to 71(FE23)]	139[48(FE13) to 241(FE28)]	18.2	7.8
SS4	Unreinforced GCLs	F	5.0	5.7	10[13(FE24) to 13(FE24)]	35[36(FE25) to 36(FE25)]	3.5	5.3
SS5	Needle-punched GCLs	*A*, *C-E*, *G-J*	19.9	39.7	58[14(FE32) to 71(FE23)]	149[107(FE19) to 241(FE28)]	18.3	7.9
SS6	Stitch-bonded GCLs	*B*	28.5	5.6	33[28(FE14) to 60(FE12)]	58[48(FE13) to 92(FE12)]	N/A	N/A
SS7	W-NW needle-punched GCLs	*A*, *C*, *G*, *I*, *J*	19.1	40.9	58[14(FE32) to 66(FE1)]	145[111(FE18) to 195(FE8)]	19.1	7.8
SS8	NW-NW needle-punched GCLs	*D*, *E*, *H*	35.0	24.5	58[23(FE19) to 71(FE23)]	172[107(FE19) to 241(FE28)]	11.3	8.7
SS9	Needle-punched GCLs without thermal-locking	*A*, *G-J*	40.5	19.5	61[14(FE32) to 66(FE1)]	149[117(FE4) to 195(FE8)]	19.7	7.7
SS10	Needle-punched GCLs with thermal-locking	*C-E*	33.2	22.7	54[23(FE19) to 71(FE23)]	159[107(FE19) to 220(FE21)]	11.8	9.0

[a]GCL sets do not consider the effect of specimen conditioning or SDR.

[b]The range includes the lowest shear strength and corresponding FE as well as the highest shear strength and corresponding FE.

[c]Upper and lower FE envelopes at the reference normal stresses were defined using the parameters presented in Table 2.

However, needle-punched GCLs with W-NW carrier geotextiles showed a lower peak shear strength than those with NW-NW carrier geotextile configurations under high normal stresses [τ_{300}(Set SS7) = 145 kPa and τ_{300}(Set SS8) = 172 kPa].

- Needle-punched GCLs that were not thermal-locked (Set SS9) showed higher peak internal shear strength under low normal stresses than those that were thermal-locked (Set SS10) [τ_{50}(Set SS9) = 58 kPa and τ_{50}(Set SS10) = 54 kPa]. However, the opposite trend is observed under high normal stress [τ_{300}(Set SS9) = 146 kPa and τ_{300}(Set SS10) = 159 kPa]. This finding suggests that thermal locking of the fiber reinforcements is more effective under high normal stresses.

Unlike comparisons of τ_p values, comparisons of τ_{ld} values among the 10 data sets can be conducted by direct comparison of the large-displacement friction angles. This is because the cohesion intercept of large-displacement shear strength envelopes is negligible (less than 20 kPa). Inspection of ϕ_{ld} values shown in Table 3 leads to the following observations regarding the internal large-displacement shear strength of GCLs:

- The large-displacement shear strength of unreinforced GCLs is consistently lower than that of reinforced GCLs [ϕ_{ld}(Set SS4) = 5.3° and ϕ_{ld}(Set SS3) = 7.8°].
- The range of large-displacement shear strength for the reinforced GCLs data sets in Table 3 is narrow (ϕ_{ld} ranging from 7.6° to 9.0°). However, the wider range of large-displacement shear strength observed for the individual failure envelopes of reinforced GCLs in Table 2 (ϕ_{ld} ranging from 4.0° to 13.7°) indicates that the variability in large-displacement shear strength should be considered.

Assessment of Shear Strength of GCLs Tested under the Same Conditioning Procedures

The assessments using τ_{50} and τ_{300} allow direct comparison among the shear strength values of different GCL types under representative normal stresses. However, shear strength characterization for design purposes requires the definition of shear strength envelopes that account for the potential effect of GCL conditioning. Comparisons between GCLs tested under similar conditions are discussed below. Additional analyses are provided by McCartney et al. (2002).

Fig. 5(a) shows the τ_p envelopes for GCLs *A* (needle-punched), *B* (stitch-bonded), and *C* (thermal-locked) tested under the same σ_n (34.5, 137.9, 310.3 kPa), t_h (168 hs), t_c (24 hs), and SDR (0.1 mm/min). Typical shear stress-displacement curves for some of these tests are shown in Fig. 2(a). Contrary to the observations made in the overall shear strength analysis, the needle-punched GCL *A* shows higher τ_p than the thermal-locked needle-punched GCL *C* for the full range of normal stresses (34.5 to 310.3 kPa). The thermal-locked GCL *C* appears to have been detrimentally affected by the long hydration time (t_h = 168 hs) under the low hydration normal stress of (σ_h = 20.7 kPa). Pullout of fibers may have occurred from the woven geotextile of GCL *C* during both hydration and shearing. The fibers in GCL *A* are typically left entangled on the surface of the woven geotextile, so significant swelling or shear displacement is required for pullout of the fibers from the carrier geotextile. On the other hand, the fibers in GCL *C* are melted together at the surfaces of the carrier geotextiles. This is consistent with the results reported by Lake and Rowe (2000), who observed that the melted fibers still pull out of the woven carrier geotextile despite thermal treatment during hydration and shearing. Consistent with trends observed using the overall shear strength assessment, the stitch-bonded GCL *B*

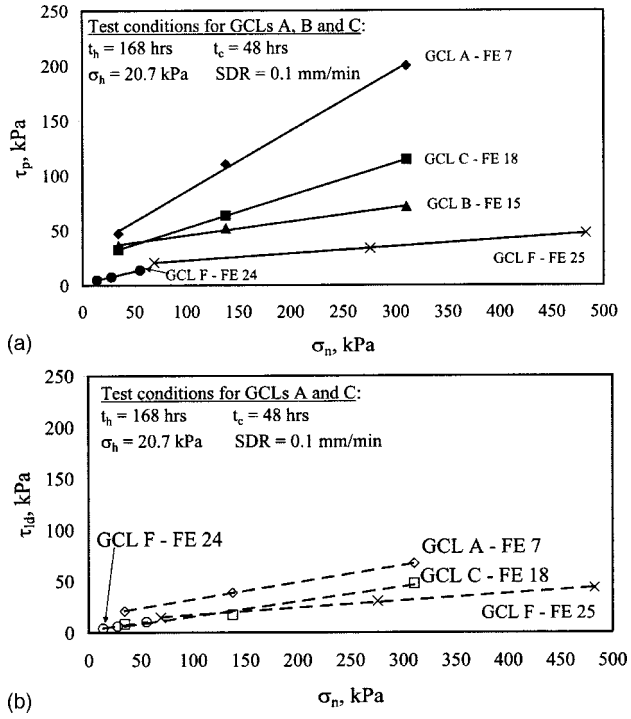

Fig. 5. Comparison of failure envelopes for needle-punched (GCL *A*), stitch-bonded (GCL *B*), thermal-locked (GCL *C*), and unreinforced (GCL *F*) GCLs: (a) peak shear strength; and (b) large-displacement shear strength. Note: When multiple shear strength results are available for a given σ_n, the data points in the figure correspond to the average shear strength value.

shows the lowest τ_p among the different reinforced GCLs. Further, consistent with observations reported by Fox et al. (1998), the continuous fiber reinforcements in GCL *B* did not break during shearing. Instead, the continuous fiber stitches tore the woven carrier geotextile while reaching comparatively large (post-peak) shear displacements. The relatively low reinforcement density (only three lines of stitching in a 305 mm wide specimen) as well as the transfer of shear stress from the stitches to the carrier geotextile during shearing probably contributed to the low τ_p of GCL *B*. Fig. 5(b) shows the τ_{ld} envelopes for the same cases. Similar to the observations for τ_p, the needle-punched GCL *A* has higher τ_{ld} than the thermal-locked GCL *C*.

Also included in Figs. 5(a and b) are the τ_p and τ_{ld} envelopes for unreinforced GCL *F*. The hydration conditioning for tests conducted under comparatively low and high σ_n (below and above approximately 60 kPa) are different. The GCL tested under low σ_n is hydrated, but shows a higher friction angle than the unhydrated GCL tested under higher σ_n. Despite the differences in GCL conditioning between the tests on unreinforced specimens, both τ_p and τ_{ld} for GCL *F* are significantly below those obtained for reinforced GCLs.

Indirect Evaluation of Pore Water Pressures Generated during Shearing

Direct measurement of pore water pressures generated during shearing poses significant experimental challenges and has not been successfully accomplished to date (Fox et al. 1998). While direct measurement of pore water pressures was beyond the scope of the commercial tests in the GCLSS database, some results provide indirect insight into the shear-induced pore water pressures. Such insight is provided by evaluation of direct shear tests conducted using different SDRs and of shear strength envelopes obtained for a wide range of σ_n. Although the behavior of GCLs under comparatively low σ_n has been reported in the technical literature, the response of GCLs under comparatively high σ_n has not been thoroughly investigated so far, probably due to experimental difficulties. Of particular interest in this study is the comparison between the behavior of GCLs tested under σ_n below and above the swell pressure of the GCL. The swell pressure has been defined as the normal stress at which the sodium bentonite in the GCL does not swell beyond its initial thickness (Petrov et al. 1997). Petrov et al. (1997) reported swell pressures ranging from 100 to 160 kPa for thermal-locked GCLs, while lower values were reported by Stark (1997) for one test conducted using a needle-punched GCL. Pore water pressures generated during shearing are indirectly investigated herein by comparing the response of tests conducted under comparatively low and high σ_n.

Evaluation of the Effect of Shear Displacement Rate

The effect of SDR on τ_p and τ_{ld} has been reported by Stark and Eid (1996), Gilbert et al. (1997), Eid and Stark (1997), Fox et al. (1998), and Eid et al. (1999). These studies, which primarily focused on the response of tests conducted under relatively low σ_n, reported an increasing τ_p with increasing SDR. The GCLSS database allows analysis of the effect of SDR on internal shear strength using tests conducted under σ_n values beyond those reported in previous studies. Fig. 6(a) shows the results of tests on GCL *A* conducted under comparatively low σ_n (50 kPa) using the same test conditions (t_h=24 hs, σ_h=σ_n, t_c=0 hs), but varying SDRs (0.01, 0.5, 1.0 mm/min). Consistent with the trend reported in past studies for tests conducted under low σ_n, the results show an increasing τ_p with increasing SDR. Fig. 6(b) shows the results of tests on GCL *A* conducted under high σ_n (520 kPa) using the same test conditions (t_h=312 hs, σ_h=496.8 kPa, t_c=48 hs), but varying SDRs (0.0015, 0.01, 0.1, 1.0 mm/min). Unlike the trend shown in Fig. 6(a) for tests conducted under low σ_n, the results in Fig. 6(b) show a decreasing τ_p with increasing SDR. The results in Figs. 6(a and b) suggest that the large-displacement shear strength appears to approach residual conditions toward the end of the test conducted with high SDR (1.0 mm/min) test while the tests conducted at lower SDRs have not reached this condition at the end of testing.

Fig. 6(c) summarizes the peak shear strength results from Figs. 6(a and b), and includes additional tests conducted to verify the repeatability of results. The value of τ_p decreases at a rate of approximately 15 kPa per log cycle of SDR for tests conducted at σ_n=520 kPa, while it increases at a rate of approximately 12 kPa per log cycle of SDR for tests conducted at σ_n=50 kPa. Varying SDR appears to have a similar effect on τ_p for the σ_n values shown in the figure (e.g., 10 to 15 kPa per log cycle). However, it should be noted that this corresponds to significant changes in τ_p for GCLs tested at σ_n=50 kPa (approximately 40% decrease per log cycle of SDR while it corresponds to smaller changes in τ_p for GCLs tested at σ_n=520 kPa (approximately 10% increase in shear strength per log cycle of SDR). Based on these observations, if design is governed by τ_p, test specification involving comparatively high are acceptable if the σ_n of interest is relatively high, as the test will lead to conservative (i.e., lower) shear

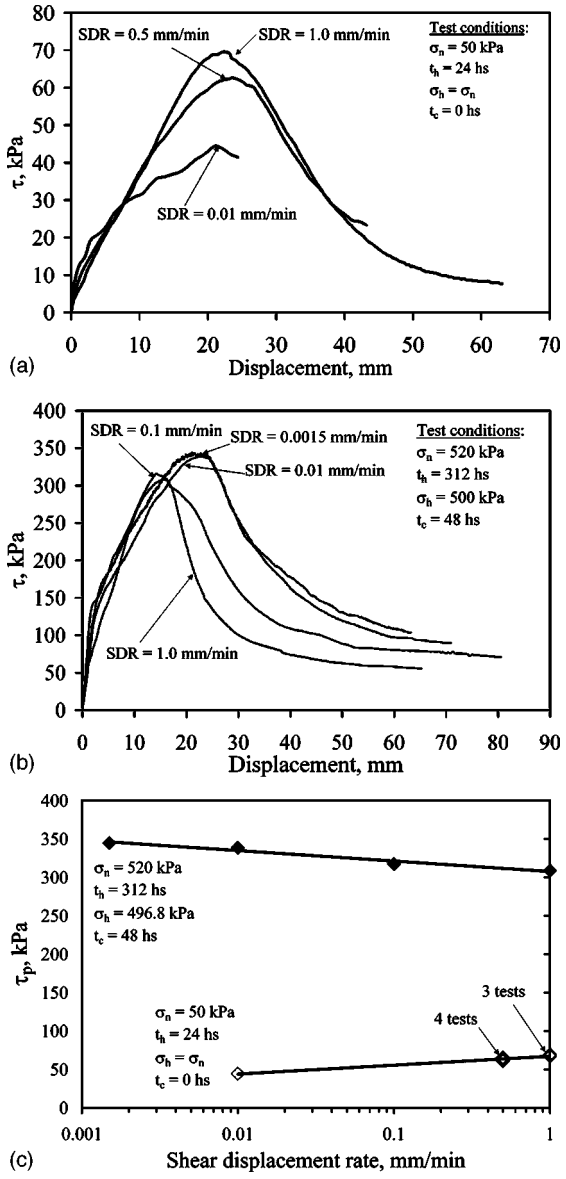

Fig. 6. Effect of shear displacement rate (SDR) on peak shear strength of needle-punched GCL *A*: (a) shear stress-displacement curves for tests under low σ_n (50 kPa); (b) shear stress-displacement curves for tests under high σ_n (520 kPa); and (c) summary trends of peak shear strength as a function of SDR

strength values. However, tests should still be specified with sufficiently low SDR (e.g., 0.1 mm/min) if the σ_n of interest is relatively low.

Explanations proposed to justify the trend of increasing τ_p with increasing SDR observed in previous studies, conducted under relatively low σ_n, have included shear-induced pore water pressures, secondary creep, undrained frictional resistance of bentonite at low water content, and SDR-dependent pullout behavior of fibers during shearing. However, the results obtained from tests conducted under both low and high σ_n suggest that the observed trends are consistent with the generation of shear-induced pore water pressures. Shear-induced pore water pressures are expected to be negative in tests conducted under low σ_n (i.e., below the swell pressure of GCLs). Consequently, increasing SDR will lead to increasingly negative pore water pressures and thus higher τ_p. This trend was also observed for tests conducted on unreinforced

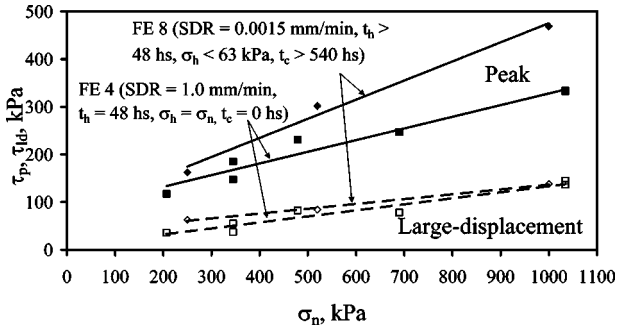

Fig. 7. Effect of shear displacement rate on the peak and large-displacement shear strength of needle-punched GCL *A*

GCLs (Gilbert et al. 1997). On the other hand, shear-induced pore water pressures are expected to be positive in tests conducted under high σ_n (i.e., above the swell pressure of GCLs). In this case, increasing SDR will lead to increasingly positive pore water pressures and thus lower τ_p.

Since no shear-induced pore water pressures are expected (positive or negative) for constant volume conditions, the same residual shear strength is anticipated for different SDRs. Eid and Stark (1999) reported that residual shear strength results were insensitive to SDRs, while Fox et al. (1998) found a slightly increasing strength with increasing SDR for a normal stress of 72.2 kPa. Although residual shear strength was not achieved for the tests reported in Figs. 6(a and b), the tests conducted using higher SDR showed post-peak shear strength loss at comparatively smaller shear displacement values. A consequence of this observation is that, if design is governed by large-displacement shear strength, direct shear tests conducted using high SDR should be adequate for preliminary internal shear strength characterization.

Indirect Evaluation of Pore Water Pressures from Shear Strength Envelopes

Fig. 7 shows FE 8, which includes three tests that were hydrated under a constant low σ_h for more than 48 hs. The normal stress was subsequently increased in stages from σ_h to σ_n during a period of over 540 hs. The specimens were finally sheared using a SDR of 0.0015 mm/min. Determination of the three data points for FE 8 required approximately one year of direct shear testing. For comparison, Fig. 7 also includes data from tests conducted using a SDR of 1.0 mm/min (FE 4). The results in this figure allow investigation of the cumulative effect of conditioning and SDR on the internal shear strength of GCL *A*. For instance, despite the different hydration and consolidation procedures of the three tests in FE 8, a well-defined linear failure envelope was obtained (R^2=0.988). Also, for the range of σ_n shown in this figure (above the swell pressure of GCLs), the trends are consistent with those observed in Fig. 6. That is, the differences in τ_p between FE 4 (SDR=1.0 mm/min) and FE 8 (SDR=0.0015 mm/min) are more significant at higher σ_n because of higher positive pore water pressures induced in FE 4. The direct shear tests corresponding to FE 4 and FE 8 appear to be approaching residual conditions toward the end of the test. The τ_{ld} envelopes suggest that the residual shear strength is approximately insensitive to the different conditioning procedures and different SDRs.

Additional insight on shear-induced pore water pressures can

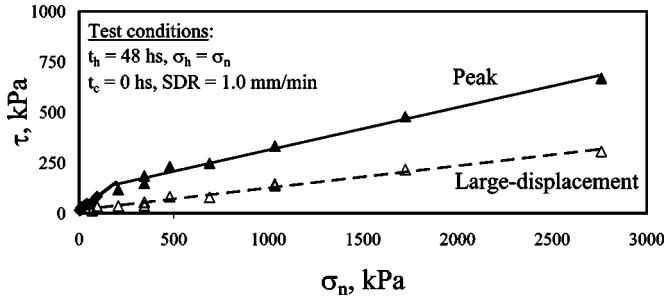

Fig. 8. Typical shear strength envelopes for needle-punched GCL *A* obtained using a wide range of σ_n

be obtained from evaluating shear strength envelopes in the GCLSS database that include tests conducted using σ_n ranging from values below to values above the swell pressure of GCLs. Fig. 8 shows τ_p and τ_{ld} results for tests on GCL *A* (FE 4) conducted using t_h=48 hs, $\sigma_h=\sigma_n$, t_c=0 hs, and SDR=1.0 mm/min. The internal shear strength envelope shown in the figure was defined using 40 direct shear tests. Some tests were conducted using σ_n as high as 2,759 kPa, which corresponds to stresses expected in bottom liners of high landfills or heap leach pads. Tests on GCLs under such high σ_n have not been reported in previous investigations. A linear envelope does not provide a good representation of τ_p over the wide range of σ_n encompassing the swell pressure of the GCL, which is consistent with nonlinear envelopes reported for GCLs (Gilbert et al. 1996; Fox et al. 1998), and for sodium montmorillonite (Mesri and Olson 1970). The GCL and unreinforced sodium bentonite are expected to be influenced by the same mechanisms when tested at normal stresses above and below the swell pressure. As shown in the figure, a bilinear FE provides a good representation of the τ_p data. Linear envelopes fit the τ_p data well for σ_n below approximately 100 kPa (c=14.4 kPa, ϕ=35.4°) and for σ_n above approximately 200 kPa (c=102.4 kPa, ϕ=11.9°). A transition zone appears to take place for σ_n ranging from 100 to 200 kPa, which is within the reported range of GCL swell pressure. The bilinear trend is not caused by a change in fiber failure mechanisms (from pullout to breakage), as the normal stress needed to induce breakage of the polypropylene fibers is well above that of typical geotechnical projects (Zornberg 2002). The τ_{ld} envelope is well represented by a linear envelope characterized by a friction angle of 6.3° and negligible cohesion intercept (c_p=16.2 kPa). Other GCLs in the database, tested under a wide range of σ_n (e.g., FE 16 and 21), show a similar bilinear τ_p response.

Consistent with the results obtained for varying SDR, the break in the bilinear trend in τ_p is in agreement with the generation of negative and positive excess pore water pressures in tests conducted using σ_n below and above the swell pressure of GCLs, respectively. The linear trend obtained for τ_{ld} a wide range of σ_n is also in agreement with the negligible pore water pressures expected under large-displacement conditions.

Variability

The number of test results in the GCLSS database is large enough to provide a basis for assessment of internal shear strength variability. Considering the composite nature of GCLs, the analyses presented herein allow both identification and quantification of different sources of shear strength variability. This information may prove relevant for reliability-based limit equilibrium analyses (McCartney et al. 2004). Potential sources of GCL internal shear strength variability include: (1) Differences in material types (type of GCL reinforcement, carrier geosynthetic), (2) variation in test results from the same laboratory (repeatability), and (3) overall material variability. In turn, the overall material variability includes more specific sources such as: (3-*a*) Inherent variability of fiber reinforcements, and (3-*b*) inherent variability of sodium bentonite. The source of variability (1) listed above is not addressed in this study since only the variability of individual GCL types is evaluated. The sources of variability (2) and (3) are assessed in this study using data presented in Table 4. This table presents a total of seven sets identified for assessment of shear strength variability. Each data set includes tests conducted using the same GCL type, same conditioning procedures, and same σ_n.

Repeatability of Test Results Obtained from the Same Laboratory

The source of variability (2) can be assessed by evaluating Sets V1 and V2 in Table 4, which includes the results of tests conducted by a single laboratory using specimens collected from a single manufacturing lot tested with the same conditioning procedures and same σ_n. Although the size of manufacturing lots is not standardized, it typically involves a set of rolls produced in a shift, day, or even week. Fig. 9 shows shear stress-displacement curves for GCL *A* specimens obtained from rolls of the same lot, which were tested by the same laboratory using the same σ_n. Although the number of tests is small, these results illustrate that good repeatability can be achieved in the stress-strain-strength response when tests are conducted in the same laboratory using same-lot specimens. As indicated by Table 4, the maximum relative difference between these tests is less than 6%, which is significantly smaller than the relative difference associated with different-lot GCLs presented in the next section.

Overall Material Variability

The source of variability (3) may be assessed by evaluating Sets V3 through V7 in Table 4. Unlike the results for Sets V1 and V2 shown in Fig. 9, the GCL specimens in Sets V3 through V7 were obtained from different manufacturing lots. For each set, Table 4 indicates the mean values for τ_p and τ_{ld} [$E(\tau_p)$ and $E(\tau_{ld})$], their standard deviations [$s(\tau_p)$ and $s(\tau_{ld})$], their coefficient of variation c.o.v. values [$s(\tau)/E(\tau)$], and the maximum relative difference. Subsets of data sets V3, V4, and V5 (V3*a* though V3*e*, V4*a* through V4*e*, and V5*a* through V5*e*), in Table 4 include the shear strength variability data corresponding to the manufacturing year of each of the GCL specimens. The maximum relative differences for Sets V3 through V7 (approximately 55%) are significantly higher than those obtained for tests using same-lot GCL specimens (6%). Sets V3, V4, and V5 include data from 141 internal shear strength tests on GCL *A* conducted using the same test conditions (t_h=168 hs, t_c=48 hs, SDR=0.1 mm/min) and three different normal stresses (σ_n=34.5, 137.9, 310.3 kPa). Evaluation of statistical information on the τ_p results for these three sets shows an increasing $s(\tau_p)$ and a relatively constant c.o.v. with increasing σ_n, which indicates that peak shear strength variability increases linearly with σ_n. The c.o.v. and maximum relative difference values are approximately 0.25 and 55%, which are significantly high values for engineering materials. Fig. 10(a) shows the τ_p envelope defined using the mean values of the 141 direct shear test results (Sets V3, V4, and V5 in Table 4). This figure

Table 4. Geosynthetic Clay Liner (GCL) Data Sets for Assessment of Shear Strength Variability

		Test conditions						Peak shear strength				Large-displacement shear strength			
GCL data set	GCL label	t_h (hs)	t_c (hs)	SDR (mm/min)	σ_n (kPa)	Year GCL manufactured	Number of tests	$E(\tau_p)$ (kPa)	$s(\tau_p)$ (kPa)	c.o.v.	Max. rel. difference[a] (%)	$E(\tau_{ld})$ (kPa)	$s(\tau_{ld})$ (kPa)	c.o.v.	Max. rel. difference[a] (%)
V1	A	24	0	0.5	48.3	1998	3	63.2	2.1	0.03	6	20.7	2.5	0.12	21
V2	A	24	0	0.5	386.1	1998	3	210.7	6.4	0.03	6	79.3	4.8	0.06	11
V3	A	168	48	0.1	34.5	1997–2003	47	35.6	10.4	0.29	64	20.6	6.27	0.30	79
V3a	*A*	*168*	*48*	*0.1*	*34.5*	*1997*	*2*	*52.1*	*4.4*	*0.08*	*11*	*8.3*	*0.0*	*0.00*	*0*
V3b	*A*	*168*	*48*	*0.1*	*34.5*	*1998*	*8*	*44.6*	*3.6*	*0.08*	*24*	*16.5*	*3.1*	*0.19*	*45*
V3c	*A*	*168*	*48*	*0.1*	*34.5*	*1999*	*9*	*47.9*	*6.1*	*0.13*	*33*	*26.0*	*9.9*	*0.38*	*75*
V3d	*A*	*168*	*48*	*0.1*	*34.5*	*2002*	*15*	*28.5*	*2.9*	*0.10*	*32*	*19.9*	*2.9*	*0.15*	*41*
V3e	*A*	*168*	*48*	*0.1*	*34.5*	*2003*	*13*	*27.3*	*5.1*	*0.19*	*42*	*21.2*	*4.5*	*0.21*	*54*
V4	A	168	48	0.1	137.9	1997–2003	47	87.4	22.2	0.25	57	39.3	8.09	0.21	75
V4a	*A*	*168*	*48*	*0.1*	*137.9*	*1997*	*2*	*114.1*	*32.7*	*0.29*	*34*	*13.8*	*0.00*	*0.00*	*0*
V4b	*A*	*168*	*48*	*0.1*	*137.9*	*1998*	*8*	*106.8*	*14.9*	*0.14*	*40*	*34.4*	*6.43*	*0.19*	*43*
V4c	*A*	*168*	*48*	*0.1*	*137.9*	*1999*	*9*	*112.7*	*15.8*	*0.14*	*34*	*43.6*	*9.16*	*0.21*	*48*
V4d	*A*	*168*	*48*	*0.1*	*137.9*	*2002*	*15*	*74.5*	*5.3*	*0.07*	*27*	*37.2*	*4.98*	*0.13*	*33*
V4e	*A*	*168*	*48*	*0.1*	*137.9*	*2003*	*13*	*68.7*	*6.0*	*0.09*	*25*	*43.9*	*4.82*	*0.11*	*29*
V5	A	168	48	0.1	310.3	1997–2003	47	166.0	33.4	0.20	51	66.6	11.75	0.18	56
V5a	*A*	*168*	*48*	*0.1*	*310.3*	*1997*	*2*	*198.9*	*60.0*	*0.30*	*35*	*39.3*	*0.00*	*0.00*	*0*
V5b	*A*	*168*	*48*	*0.1*	*310.3*	*1998*	*8*	*203.0*	*21.0*	*0.10*	*27*	*63.9*	*10.06*	*0.16*	*43*
V5c	*A*	*168*	*48*	*0.1*	*310.3*	*1999*	*9*	*197.2*	*23.2*	*0.12*	*33*	*67.8*	*15.94*	*0.24*	*53*
V5d	*A*	*168*	*48*	*0.1*	*310.3*	*2002*	*15*	*146.5*	*12.8*	*0.09*	*29*	*61.5*	*7.99*	*0.13*	*34*
V5e	*A*	*168*	*48*	*0.1*	*310.3*	*2003*	*13*	*138.9*	*8.8*	*0.06*	*23*	*75.3*	*5.70*	*0.08*	*18*
V6	A	48	0	1.0	9.6	1997	18	31.1	5.8	0.19	55	N/A	N/A	N/A	N/A
V7	F	24	0	1.0	9.6	1999	6	3.9	0.7	0.19	35	3.0	0.5	0.15	35

[a]Maximum relative difference $=[(\max \tau_p - \min \tau_p)/\max \tau_p] \times 100\%$.

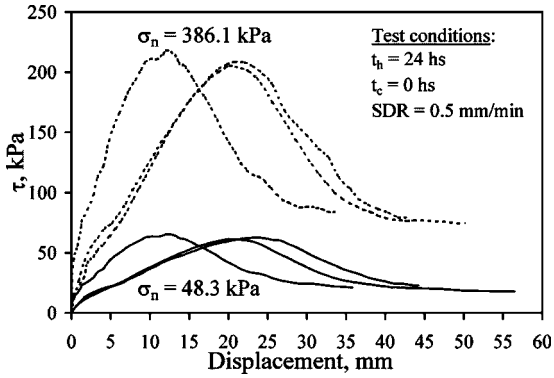

Fig. 9. Repeatability of test results on needle-punched GCL *A* specimens from rolls taken from the same lot

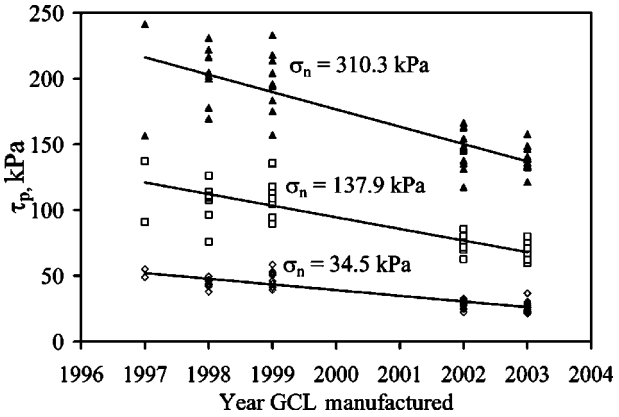

Fig. 11. Peak shear strength of GCL *A* for different manufacturing years

illustrates the significant scatter of results from tests conducted using the same GCL type and test conditions, but using specimens from different GCL *A* lots. Fig. 10(b) shows idealized normal probability density distributions for τ_p at each σ_n, obtained using the mean and standard deviation for the shear strength data of Sets V3, V4, and V5. These probability distributions quantify statistical information on τ_p, which is useful for reliability-based design. Table 4 also includes statistical information regarding τ_{ld}. Although τ_{ld} may not be fully representative of the residual shear strength, the c.o.v. of τ_{ld} is relatively high (up to 0.30), which indicates that the variability in large-displacement shear strength is not less significant than that of peak shear strength.

The 141 GCL specimens in Sets V3 through V5 were received between January 1997 and May 2003. The c.o.v. and maximum relative difference for each of the subsets of Sets V3 to V5 are typically lower each year than for the overall multiyear data sets. For example, the overall c.o.v. for Set V3 is 0.29 while the c.o.v. values for Subsets V3*a* through V3*d* range from 0.08 to 0.19. Fig. 11 shows the shear strength variability for each manufacturing year. A slight decreasing trend in the mean value of the peak shear strength is observed with each subsequent GCL manufacturing year. However, a decreasing trend in the standard deviation value of the peak shear strength is also observed with each subsequent GCL manufacturing year for high normal stresses (e.g., σ_n = 137.9 and 310.3 kPa), which may reflect an improvement over time of manufacturing quality assurance programs.

Set V6 in Table 4 includes variability data from a set of 19 direct shear tests conducted using the same GCL tested in Sets V3 through V5 (GCL *A*, manufactured in 1997), but different test conditions (t_h = 48 hs, t_c = 0 hs, SDR = 1.0 mm/min, σ_n = 9.6 kPa). The c.o.v. and maximum relative difference for Set V6 are similar to those for Sets V3 through V5 despite the shorter time allowed for conditioning (t_h = 24 hs). This suggests that specimen conditioning is not a major source of inherent material variability.

Inherent Variability of Fiber Reinforcements

Peel strength results have been reported to provide an index of the density (and possibly the contribution) of fiber reinforcements in needle-punched GCLs (Heerten et al. 1995, Eid and Stark 1997). Consequently, an assessment is made herein of the usefulness of peel strength as an indicator of the fiber contribution to GCL internal shear strength. If useful, the peel strength variability would be an indicator of the contribution of fibers to the variability of GCL shear strength [source of variability (3-*a*)]. The peel strength test (ASTM 1999) involves clamping the carrier geotextiles of a 100 mm wide unhydrated GCL specimen, and applying a force normal to the GCL plane until separating (or peeling) the geotextiles. It should be noted that the peel strength test mobilizes the fibers in a manner that may not be representative of the conditions in which the fibers are mobilized during shearing.

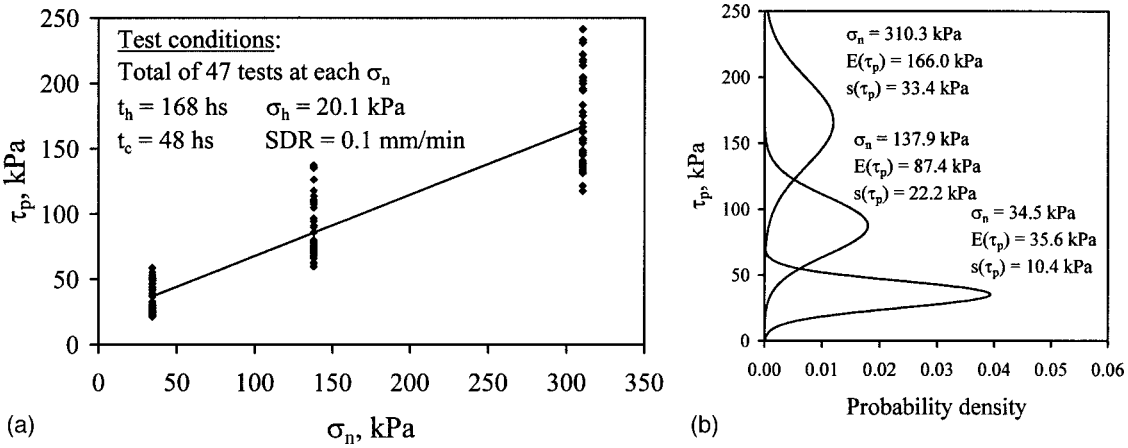

Fig. 10. Variability of peak shear strength results obtained using needle-punched GCL *A* specimens from different lots, tested using same conditioning procedures and σ_n: (a) τ_p envelope; and (b) normal distributions for τ_p at each σ_n

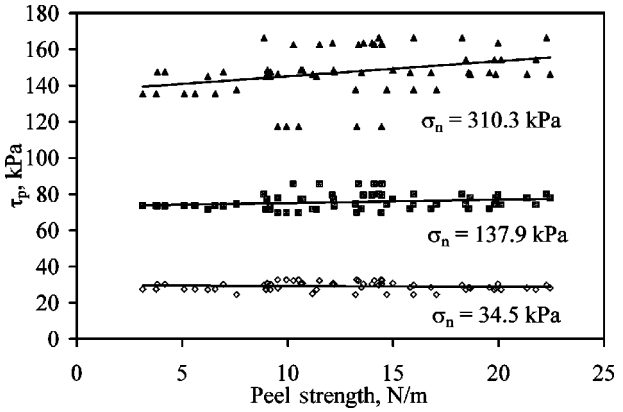

Fig. 12. Relationship between peel strength and τ_p for needle-punched GCL *A*

A total of 75 peel strength tests were conducted using GCL *A* specimens manufactured in 2002. Specifically, five tests were conducted using GCL *A* specimens from 15 rolls (different lots) manufactured in 2002 used for the test results presented in Fig. 10 (Sets V3 through V5 in Table 4). The peel strength specified by the GCL *A* manufacturer is 6.5 N/m. However, peel strength results varied significantly (from 4.3 to 22.5 N/m), with a mean of 12.5 N/m and a standard deviation of 5.51 N/m. The relationship between peel strength and τ_p obtained using GCL specimens collected from these 15 rolls is shown in Fig. 12. Although a slightly increasing trend of peel strength with increasing τ_p can be observed at high σ_n, the results suggest that τ_p is not very sensitive to the peel strength. This is consistent with results reported by Richardson (1997). Consequently, no conclusion can be drawn regarding the effect of the inherent variability of peel strength on the variability of the fiber contribution to GCL internal shear strength [source of variability (3-*a*)]. Instead, these results suggest that mobilization of fiber reinforcement in peel strength tests may not be representative of the mobilization of fibers in shear tests. Accordingly, the peel strength appears not to be a good indicator of the contribution of fibers to τ_p.

Inherent Variability of Sodium Bentonite

The source of variability (3-*b*) may be assessed by evaluating the internal shear strength variability of unreinforced GCLs. Set V7 (Table 4) includes variability data from six direct shear tests conducted using an unreinforced GCL (GCL *F*). The tests were conducted using a relatively low σ_n (9.6 kPa) and the same test conditions (t_h=24 hs, t_c=48 hs, SDR=1.0 mm/min). The variability of direct shear test results for unreinforced GCLs is useful to assess the variability of the bentonite shear strength contribution to the shear strength of reinforced GCLs. It should be noted that adhesives are mixed with the sodium bentonite, but they have been reported to have little effect on the GCL internal shear strength once hydrated (Eid and Stark 1997). The c.o.v. and maximum relative difference of the τ_p obtained for Set V7 using unreinforced GCLs is similar to that obtained for Sets V3 through V6 using reinforced GCLs (c.o.v. of approximately 0.20). In particular, the reinforced GCLs (GCL *A*) in Set V6 were tested under the same σ_n and similar conditioning procedures as the unreinforced GCLs in Set V7. Even though the internal shear strength variability has been attributed mainly to the fibers, the similar magnitude of variability observed in the unreinforced GCLs suggests that the variability of the sodium bentonite [source of variability (3-*b*)] is also relevant.

Conclusions

A database of 414 GCL internal shear strength tests was analyzed in this study. The data were obtained from large-scale (305 mm by 305 mm) direct shear tests conducted by a single laboratory over a period of 12 years using procedures consistent with current testing standards. Shear strength parameters were defined to evaluate the effect of GCL type, indirectly quantify the effect of pore water pressures, and assess sources of internal shear strength variability. The following conclusions can be drawn from this study:

1. Comparisons were made between shear strength values obtained for normal stresses representative of cover and bottom liners (50 and 300 kPa, respectively). This evaluation indicates a high scatter in peak internal GCL shear strength. Reinforced GCLs were observed to have significantly higher peak shear strength than unreinforced GCLs. Stitch-bonded GCLs were observed to have lower peak shear strength than needle-punched GCLs. Needle-punched GCLs with NW-NW GCL carrier geotextile configurations were observed to have higher peak shear strength than those with W-NW GCL carrier geotextiles. Needle-punched GCLs without thermal locking were observed to have higher peak shear strength at low normal stresses than those with thermal locking, but the opposite trend was observed at high normal stresses.
2. Unreinforced GCLs were observed to have lower large-displacement shear strength than reinforced GCLs.
3. Stitch-bonded GCLs showed a higher displacement at peak than the other reinforced GCLs.
4. Thermal locking of needle-punched GCLs was detrimentally affected by long hydration periods under low hydration normal stresses. Thermal locking was observed to be effective at high normal stresses.
5. The peak shear strength of reinforced GCLs was observed to increase with increasing SDR for tests conducted under low σ_n, while the opposite trend was observed under high σ_n. This behavior is consistent with the generation of negative shear-induced pore water pressures under low σ_n (below the swell pressure) and of positive pore water pressures under high σ_n. Consequently, if design is governed by τ_p, test specification involving comparatively high SDR are acceptable if the σ_n of interest is relatively high, as the test will lead to conservative (i.e., lower) shear strength values. However, tests should still be specified with sufficiently low SDR (e.g., 0.1 mm/min) if the σ_n of interest is relatively low.
6. Large-displacement shear strength was achieved at smaller shear displacements in tests conducted using comparatively large SDRs. consequently, tests with high SDR should be adequate if design is governed by τ_{ld}.
7. Peak shear strength results obtained over a wide range of σ_n (up to 2,759 kPa) defined bilinear failure envelopes in which a break was defined for normal stresses consistent with the swell pressure of GCLs.
8. Good repeatability of results was observed for tests conducted by the same laboratory using GCL specimens from the same manufacturing lot. However, significant variability was observed for tests conducted using GCL specimens obtained from different lots over a period of 7 years. Nonetheless, the variability among GCLs manufactured in a single year is less than that observed over the 7 year period.
9. The shear strength variability, quantified by the c.o.v. and maximum relative difference, was observed to increase lin-

early with σ_n, but was found to be insensitive to specimen conditioning procedures.

10. Peel strength results showed a relatively high variability. However, the τ_p was found not to correlate well with the peel strength. Consequently, no conclusions can be drawn regarding the effect of the variability of peel strength on the variability of GCL internal shear strength.
11. The c.o.v. of unreinforced GCLs was observed to be similar to that of reinforced GCLs, indicating that the inherent variability of sodium bentonite is a relevant source of reinforced GCL shear strength variability.

Acknowledgments

The writers thank SGI Testing Services and GeoSyntec Consultants for making available the experimental results analyzed in this study. Review provided by Dr. Paul Sabatini and Dr. Neven Matasovic of GeoSyntec Consultants is appreciated. The views expressed in this paper are solely those of the writers.

References

American Society of Testing and Materials. (1998). "Standard test method for determining the internal and interface shear resistance of geosynthetic clay liner by the direct shear method." *ASTM D6243*, West Conshohocken, Pa.

American Society of Testing and Materials. (1999). "Standard test method for determining average bonding peel strength between the top and bottom layers of needle-punched geosynthetic clay liners." *ASTM D6496*, West Conshohocken, Pa.

Eid, H. T., and Stark, T. D. (1997). "Shear behavior of an unreinforced geosynthetic clay liner." *Geosynthet. Int.*, 4(6), 645–659.

Eid, H. T., Stark, T. D., and Doerfler, C. K. (1999). "Effect of shear displacement rate on internal shear strength of a reinforced geosynthetic clay liner." *Geosynthet. Int.*, 6(3), 219–239.

Fox, P. J., Rowland, M. G., and Scheithe, J. R. (1998). "Internal shear strength of three geosynthetic clay liners." *J. Geotech. Geoenviron. Eng.*, 124(10), 933–944.

Heerten, G., Saathoff, F., Scheu, C., von Maubeuge, K. P. (1995) "On the long-term shear behavior of geosynthetic clay liners (GCLs) in capping sealing systems." *Proc., Int. Symposium Geosynthetic Clay Liners*, 141–150.

Helsel, D. R., and Hirsh, R. M. (1991). *Statistical methods in water resources*, United States Geologic Survey.

Gilbert, R. B., Fernandez, F. F., and Horsfield, D. (1996). "Shear strength of a reinforced. clay liner." *J. Geotech. Eng.*, 122(4), 259–266.

Gilbert, R. B., Scranton, H. B., and Daniel, D. E. (1997). "Shear strength testing for geosynthetic clay liners." *Testing and acceptance criteria for geosynthetic clay liners, ASTM STP 1308*, L. W. Well, ed., ASTM, Philadelphia, 121–138.

Lake, C. G., and Rowe, R. K. (2000). "Swelling characteristics of needle-punched, thermal treated geosynthetic clay liners." *Geotext. Geomembr.*, 18, 77–101.

McCartney, J. S., Zornberg, J. G., and Swan, R. (2002). "Internal and interface shear strength of Geosynthetic Clay Liners (GCLs)." *Geotech. Research Rep.*, Dept. of Civil, Environmental, and Architectural Engineering, Univ. of Colorado at Boulder.

McCartney, J. S., Zornberg, J. G., Swan, R. H., Jr., and Gilbert, R. B. (2004). "Reliability-based stability analysis considering GCL shear strength variability." *Geosynthet. Int.* 11(3), 212-232.

Mesri, G., and Olson, R. E. (1970). "Shear strength of montmorillonite." *Geotechnique*, 20(3), 261–270.

Petrov, R. J., Rowe, R. K., and Quigley, R. M. (1997). "Selected factors influencing GCL hydraulic conductivity." *J. Geotech. Geoenviron. Eng.*, 123(8), 683–695.

Richardson, G. N. (1997). "GCL internal shear strength requirements." *Geosynth. Fabric Rep.*, March, 20–25.

Stark, T. D. (1997). "Effect of swell pressure on GCL cover stability." *Testing and Acceptance Criteria for Geosynthetic Clay Liners, ASTM STP 1308*, L. W. Well, ed., American Society for Testing and Materials, Philadelphia, 30–44.

Stark, T. D., and Eid, H. T. (1996). "Shear behavior of a reinforced geosynthetic clay liner." *Geosynthet. Int.*, 3(6), 771–785.

Stoewahse, C., Nixon, N., Jones, D. R. V., Blumel, W., and Kamugisha, P. (2002). "Geosynthetic interface shear behavior." *Ground Eng.*, February, 35–41.

Zornberg, J. G. (2002). "Discrete framework for limit equilibrium analysis of fiber-reinforced soil." *Geotechnique*, 52(8), 593–604.